Chapter 26

LOW NOISE DESIGN

Michiel H. L. Kouwenhoven, Arie van Staveren, Wouter A. Serdijn and Chris J. M. Verhoeven
Electronics Research Laboratory/DIMES, Delft University of Technology, the Netherlands

26.1. Introduction

Noise plays an important role in analog circuit design, since it is involved in many design trade-offs. For this reason, it asks for a careful treatment by the designer; at one side, circuits have to realize the required signal processing, at the other side, the circuit components produce noise that corrupts the information.

A frequently applied approach to handle such conflicting requirements is to establish an acceptable trade-off between the various design requirements. Finding such a trade-off, however, is usually a difficult and time-consuming task that for large circuits can only be found through numerical optimization, for example, as in [1].

An often more attractive and effective approach is to eliminate the conflict between design requirements, such that each of them can be optimized separately. Such an "orthogonalization" of requirements can be achieved by assigning conflicting requirements to different parts of the circuit. These can then be separately optimized. The strength of this approach is that the design procedure becomes straightforward, without the need of complicated optimization techniques.

In this chapter, we will show how the noise performance of various types of circuits can be improved by elimination of trade-offs between noise and other requirements. Section 26.2 briefly reviews some useful tools for the analysis of the circuit noise behavior. Sections 26.3–26.5 discuss the design techniques to minimize the noise level in amplifiers, harmonic oscillators and relaxation oscillators, respectively.

26.2. Noise Analysis Tools

Noise analysis tools are indispensable in optimization of the noise behavior of circuits. They reveal the dominant causes of the circuit noise production, and also indicate possibilities to minimize it. In this section, we briefly review some noise analysis techniques that are very useful in the synthesis of low noise circuits.

C. Toumazou et al. (eds), Trade-Offs in Analog Circuit Design: The Designer's Companion, 747–785.

Generally, the purpose of a noise analysis is to determine the equivalent input/output Signal-to-Noise Ratio (SNR) of a circuit. To this extent, all noise produced by the various circuit components is thought to be concentrated into a single noise source, the so-called "equivalent" noise source. The power contents of this source equal the noise power produced by the entire circuit, and can be obtained through standard techniques [2,3]. The remainder of this section will concentrate on the determination of this equivalent noise source from the various circuit noise processes.

26.2.1. Equivalent Noise Source

The equivalent input noise source replaces all other noise sources in the circuit; once this source is obtained, the remainder of the circuit can be considered "noise free". Consequently, it may be viewed as the resultant of transforming all circuit noise sources to a single position, as illustrated by Figure 26.1.

The noisy circuit is represented as a noise-free multi-port, connected to independent noise sources $v_{n,2i}$ and $i_{n,2i+1}$ that represent the various circuit noise processes. The equivalent noise source $e_{n,eq}$ is connected to one of the circuit ports (usually the input or output) and equals the resulting voltage/current at this port due to the noise sources $v_{n,2i}$ and $i_{n,2i+1}$. Usually, the circuit behaves (small-signal) linear with respect to the noise, such that the (time-domain) transfer from $v_{n,2i}$ and $i_{n,2i+1}$ to $e_{n,eq}$ can be represented by an impulse response:

$$e_{n,eq}(t) = \sum_{i=1}^{n} h_{2i} * v_{n,2i}(t) + \sum_{k=0}^{m} h_{2k+1} * i_{n,2k+1}(t) \qquad (26.1)$$

where "*" denotes a convolution. Consequently, the noise transformation essentially consists of calculating the impulse responses $h_k(\tau)$, or equivalently the frequency transfers $H_k(j\omega)$. This can be done through combination of the four types of transforms discussed below.

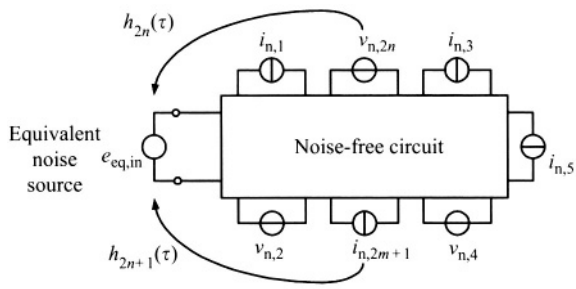

Figure 26.1. Representation of noisy circuit as a noise-free multi-port network, connected to multiple noise sources.

26.2.2. Transform-I: Voltage Source Shift

The voltage source shift (V-shift) is a transform that enables to move (noise) voltage sources through the circuit without changing the maze equations defined by the Kirchhoff Voltage Law (KVL). Its principle is visualized in Figure 26.2.

The original (noise) source v_n is shifted out of the branch between the nodes 1,4 into the two other branches connected to node 4; the ones between 2,4 and 3,4. In order to guarantee that the KVLs of the mazes I, II and III, associated to node 4 remain unchanged, the new sources $v_{n,1}$ and $v_{n,2}$ have to be exactly equal to each other, that is, fully correlated, and to the original source v_n.

26.2.3. Transform-II: Current Source Shift

The dual transform of the V-shift is the I-shift, which allows moving current (noise) sources through the circuit without changing the nodal equations defined by the Kirchhoff Current Law (KCL). The principle is depicted in Figure 26.3.

The original (noise) current source i_n is redirected from the branch between nodes 1,2 through the sources $i_{n,1}$ and $i_{n,2}$ between nodes 1,3 and 2,3. In order to keep the KCLs of the nodes 1, 2 and 3 unchanged, $i_{n,1}$ and $i_{n,2}$ have to be exactly equal to each other (fully correlated) and to i_n.

26.2.4. Transform-III: Norton–Thévenin Transform

The equivalence of the well-known theorems of Norton and Thévenin can be used to transform a (noise) current source into a (noise) voltage source and vice versa. This type of transform does essentially not move sources through

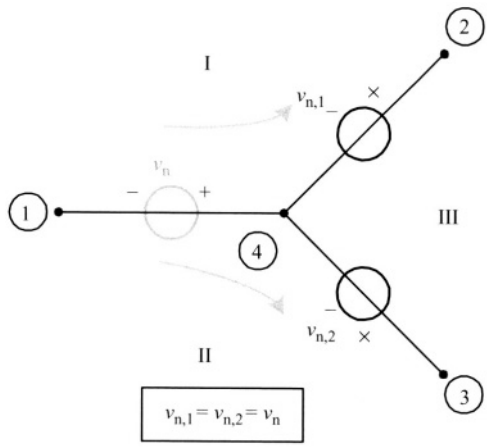

Figure 26.2. V-shift transform.

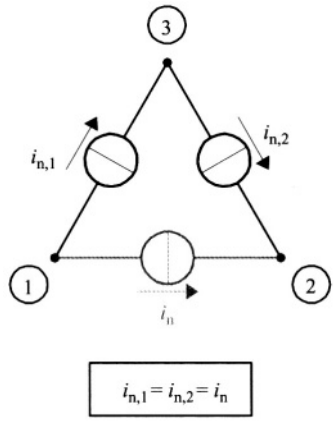

Figure 26.3. I-shift transform.

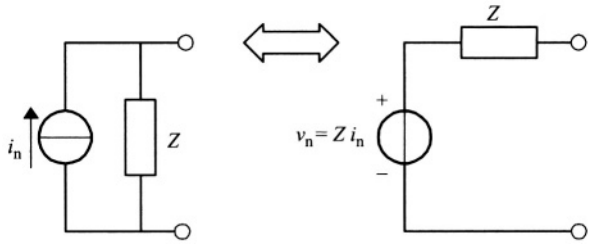

Figure 26.4. Norton–Thévenin transform.

the amplifier network, but is used to switch between the V-shift and I-shift. An example of its application is depicted in Figure 26.4.

The current source i_n and the voltage source v_n have a one-to-one correspondence through the impedance Z. They are fully correlated. Note that this transformation does change the KVLs and KCLs of the circuit; it exchanges a circuit branch for a circuit node, and vice versa. For this reason, the Norton–Thevenin transform, in combination with the V-shift and I-shift can be used to eliminate a voltage source from a maze, or a current source from a node.

26.2.5. Transform-IV: Shift through Twoports

The three transformations we have considered so far are all concerned with two-terminal elements (oneports) only. If a network consists entirely of such elements, these three transforms are all we need to determine the equivalent input noise.

Many circuits, however, also contain elementary twoports, controlled sources (included in transistor models) or a nullor, that cannot be replaced

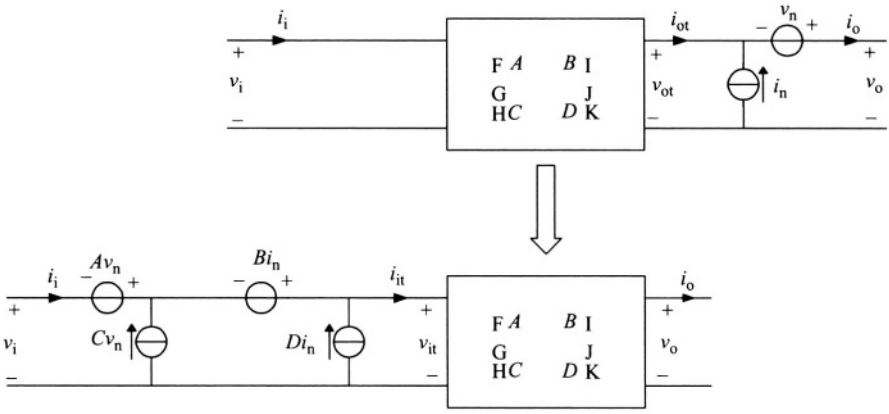

Figure 26.5. Transformation of noise sources through a twoport.

by any combination of oneports. For such networks, we need an additional transform: the twoport shift. This transformation is illustrated by Figure 26.5.

The output voltage v_o and the output current i_o of the twoport are mutilated by a noise voltage v_n and noise current i_n, respectively, as depicted in the upper part of the figure. The purpose of the twoport shift transform is to obtain the equivalent input noise source that yields this output noise. The result depicted in the lower part of the figure is easily obtained from the chain matrix equation for the twoport,

$$\begin{pmatrix} v_{it} \\ i_{it} \end{pmatrix} = \begin{pmatrix} A & B \\ C & D \end{pmatrix} \begin{pmatrix} v_{ot} \\ i_{ot} \end{pmatrix} \tag{26.2}$$

and substitution of v_i, i_i, v_o, i_o, v_n and i_n. Observe that the output noise voltage source v_n is transformed into an input noise voltage source Av_n and a noise current source Cv_n that are fully correlated. Likewise, the output noise current source i_n transforms into an input noise voltage source Bi_n and an input noise current source Di_n.

26.3. Low-Noise Amplifier Design

Amplifiers are the hearts of many electronic circuits and systems. Besides their direct use to increase the power content of small information signals, in order to make them less vulnerable to noise, they are also used as key building blocks in, for example, filters, oscillators and bandgap references.

The main trade-off to be made in amplifier designs is among the amplifier noise production, distortion generation and its bandwidth. Especially when a high-performance level is required, it is difficult (or even impossible) to satisfy all requirements simultaneously within one amplifier stage. For this reason,

we will attempt to make these requirements "orthogonal" and optimize them separately. A particularly suitable concept that enables such an "orthogonalization" is overall negative feedback; it localizes the various design requirements in different parts of the amplifier circuit. This section will, therefore, focus on the design of low-noise negative feedback amplifiers.

26.3.1. Design of the Feedback Network

Essentially, a negative feedback amplifier consists of two parts; an active part that provides the amplification, and a feedback network that accurately fixes the overall gain to a predefined value. The active part consists of a combination of transistors that approximates a "nullor"; a circuit theoretical twoport element with infinite gain (all elements of its chain matrix equal zero).

In theory, the nullor and the feedback network establish complete orthogonality between the overall amplifier gain at one side, and requirements with respect to noise, distortion and bandwidth at the other side. The feedback network only fixes the overall gain, and has no effect on the noise, distortion or bandwidth. The nullor implementation completely determines the noise, distortion and bandwidth of the amplifier and has no influence on the overall gain. Further, inside the nullor, the noise, distortion and bandwidth requirements can be made orthogonal by localizing them to different stages, as will be discussed in Subsection 26.3.2. The idealized amplifier configurations that establish such a perfect orthogonalization, consisting of a nullor and feedback networks of ideal transformers and gyrators are depicted in Figures 26.6 and 26.7.

The amplifier in Figure 26.6 comprises all four possible feedback loops. It realizes an accurate power gain and has an independently configurable input and output impedance. Figure 26.7 depicts the four types of ideal single-loop amplifiers. The ideal transformers and gyrators in these configurations only determine the amplifier gain, and have no effect on the noise, distortion or bandwidth.

Unfortunately, ideal transformers and gyrators are not available, such that, in practice, a designer has to resort to amplifiers using impedance feedback networks. Figure 26.8 depicts the impedance feedback amplifiers corresponding to the ideal types in Figure 26.7.

An important difference with the ideal transformer–gyrator configurations is that the orthogonality between the design requirements in these configurations is no longer perfect. The feedback impedances disturb the orthogonality in three different ways:

- They generally produce noise.
- They magnify the noise produced by the nullor.
- They increase the distortion and reduce the bandwidth.

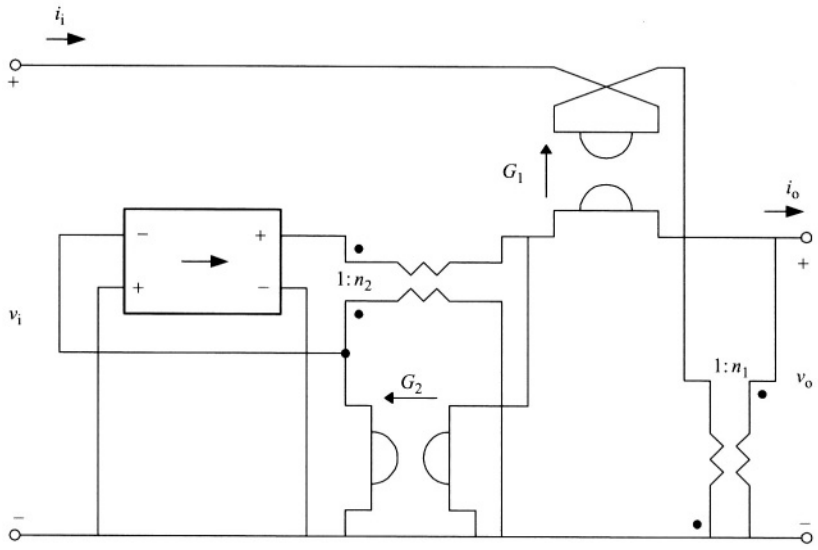

Figure 26.6. Ideal amplifier configuration comprising all possible feedback loops.

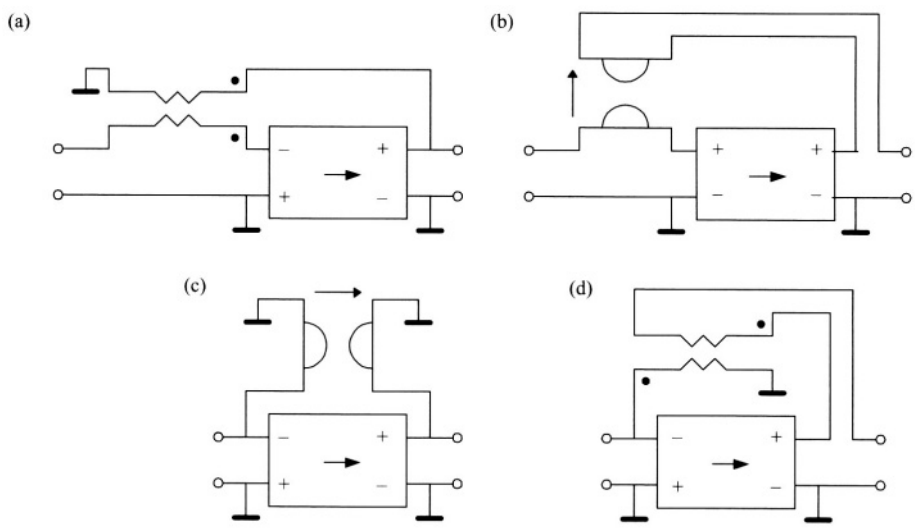

Figure 26.7. The four types of ideal single-loop amplifiers. (a) Voltage amplifier, (b) transconductance amplifier, (c) transimpedance amplifier and (d) current amplifier.

Noise production by the feedback network. This way of affection is rather obvious. If the feedback network contains resistors, it will produce noise such that the amplifier noise production is no longer completely localized inside the nullor.

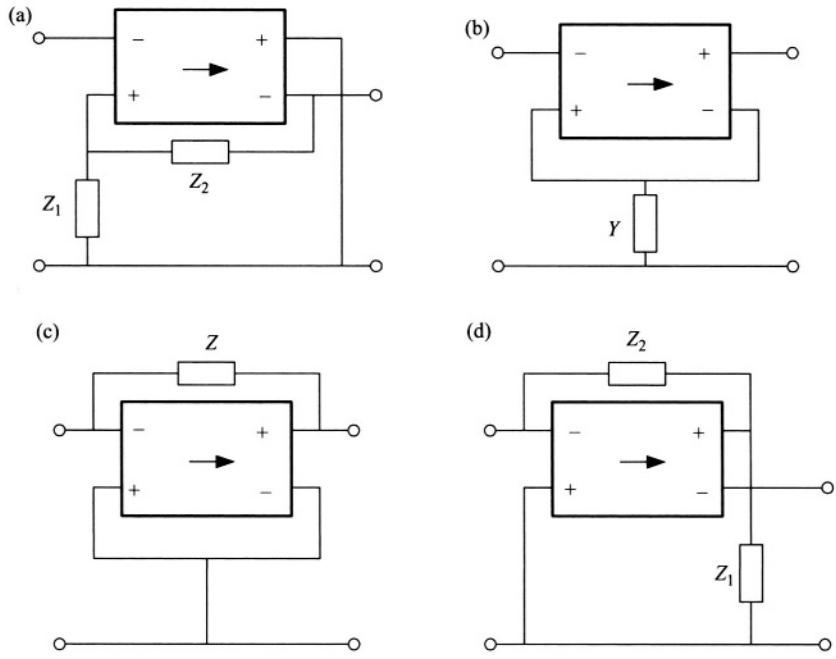

Figure 26.8. Single-loop amplifier configurations using impedance feedback (a) voltage amplifier, (b) transconductance amplifier, (c) transimpedance amplifier and (d) current amplifier.

Magnification of nullor noise. This contribution is less obvious. Even when the impedance feedback network contains no resistors (i.e. consists of capacitors and inductors), it still increases the amplifier noise by magnifying the nullor noise. The voltage amplifier in Figure 26.9 illustrates this effect.

The noise produced by the nullor is represented by the noise sources v_n and i_n. Using the analysis tools discussed in Section 26.2, the equivalent input noise source of the complete amplifier, $v_{n,eq}$ is found to equal:

$$v_{n,eq} = v_n + \left(Z_s + \frac{Z_1 Z_2}{Z_1 + Z_2} \right) i_n \tag{26.3}$$

This expression clearly shows that the feedback impedances Z_1 and Z_2 increase ("magnify") the contribution of i_n to the equivalent input noise source $v_{n,eq}$, even when they are capacitors or inductors. In an amplifier using transformer feedback, i_n would contribute to $v_{n,eq}$ through R_s only. It can be shown for the configurations in Figure 26.8 that the feedback network has the same effect on the amplifier noise as an impedance, equal to the output impedance, of the feedback network that is connected in series/parallel with the input signal

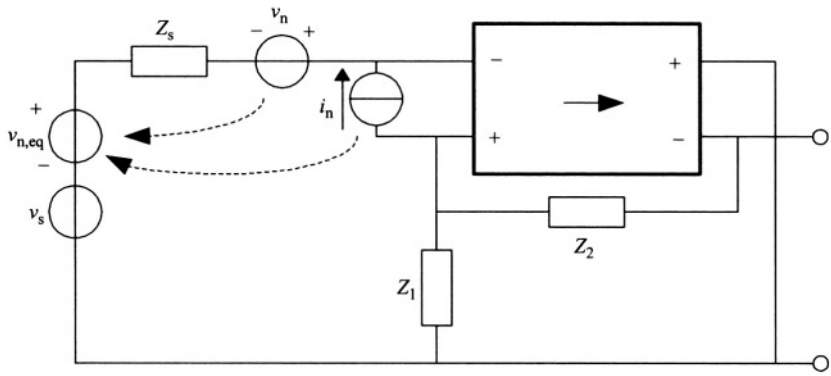

Figure 26.9. Magnification of the nullor noise by the feedback impedances.

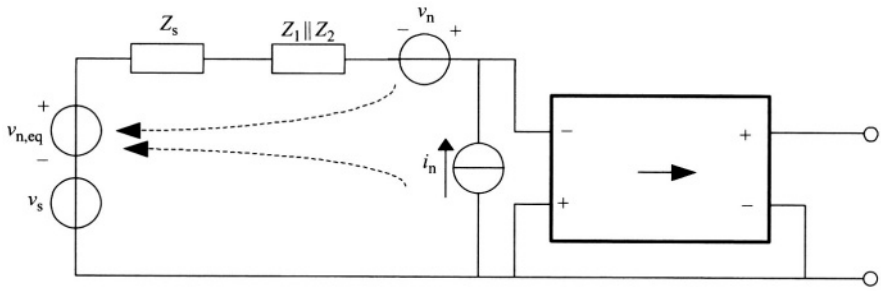

Figure 26.10. Equivalent circuit of the voltage amplifier in Figure 26.9 with respect to noise.

voltage/current source. For example, the result given by equation (26.3) could also be obtained from Figure 26.10, which is equivalent to Figure 26.9 with respect to noise.

Generally, these equivalent circuits provide a very efficient "short-cut" in the analysis of the amplifier noise behavior.

Distortion increment and bandwidth reduction. Impedance feedback networks affect the amplifier distortion and bandwidth due to the fact that they consume power. Their input impedance loads the output stage of the nullor, which increases the distortion (the nullor output stage has to deliver more power) and reduces the bandwidth (the loop-gain is reduced). As a consequence, a "residual" trade-off between noise, distortion and bandwidth remains present. For example, a low value of the feedback impedances Z_1 and Z_2 is beneficial in a voltage amplifier with respect to noise. At the same time, however, this may also cause a low value of the feedback network input impedance

$Z_1 + Z_2$, which deteriorates the distortion and bandwidth. Often, the increase of distortion and reduction of bandwidth can be repaired by increasing the bias current of the nullor output stage (increase power consumption). However, it is clear that the feedback impedances should not be chosen much smaller (larger) than is necessary to match the noise requirements.

26.3.2. Design of the Active Part for Low Noise

The nullor implementation has to comply simultaneously with the requirements with respect to noise, distortion and bandwidth. To achieve this, we "orthogonalize" the requirements by confining them to different stages inside the nullor in the following way.

Since small signals are more vulnerable to noise than large ones, it is likely that the amplifier input has a dominant influence on the noise performance; the power contents of the information signal is minimum here. Therefore, it makes sense to design the nullor input stage for minimum noise, and assure that the noise contribution of other stages is negligible. Similarly, the distortion is likely to be dominated by the output stage, since the signal levels are maximal there. By proper design, it can be assured that all distortion is confined to the nullor output stage. Similarly, the bandwidth requirements can be localized into intermediate stages [2]. In this section, we concentrate on the design of the input stage for low noise.

The input stage of the nullor in a low-noise amplifier has to comply with two requirements:

- It has to assure orthogonality between noise and the other requirements.
- Its own noise production should be minimal.

To assure orthogonality, the gain of the nullor input stage should be made as large as possible. This was noticed already by Friis in 1944 [4] in conjunction with repeaters for telegraph lines. It also directly follows from the twoport transformation discussed in Section 26.2 as illustrated by Figure 26.11.

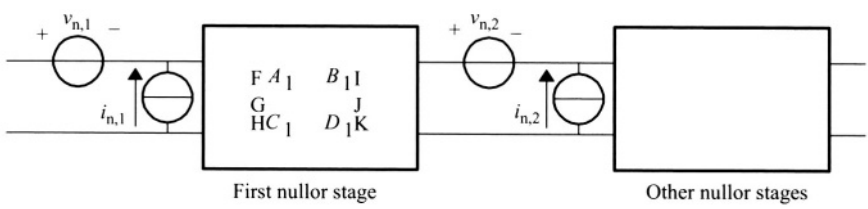

Figure 26.11. Assuring orthogonality with respect to noise by maximization of the gain of the input stage.

The twoport on the left of this figure represents the nullor input stage, while the one on the right represents the other stages. The equivalent input noise of these stages, represented by $v_{n,2}$ and $i_{n,2}$ transforms to the amplifier input through the chain parameters of the input stage, according to Figure 26.5. Their contribution to the equivalent amplifier input noise vanishes when all chain parameters of the input stage equal zero, that is, when the gain of the input stage is infinite. The transistor stage that best approximates this behavior is the common source (CS) stage for MOSFETS/JFETS, or the common emitter (CE) stage for bipolar transistors. These are the only stages that do not contain local feedback, like the emitter/source follower $(A \approx 1)$ or current follower $(D \approx 1)$.

In order to assure that the noise production of the input stage itself is minimum, it should clearly not contain local impedance feedback, such as in a shunt or series stage. The remaining options are a CE/CS stage, an emitter/source follower and a current follower. The noise production of these three stages are almost identical. Since the chain parameters of the CE/CS stage are significantly smaller than one or more chain parameters of the other ones, it is by far the preferred choice to implement the input stage. In some cases, a stage derived from the CE/CS-stage (like a differential pair) is also suitable; their chain parameters differ only slightly from that of the CE/CS stage.

26.3.3. Noise Optimizations

After selection of the feedback network and the nullor input stage, there are still some degrees of freedom left to optimize the amplifier noise performance. These optimizations will be discussed below. In general, one or more of the following three types of optimizations can be applied:

- Noise matching to the source.
- Optimization of the bias current of the first stage.
- Connecting several input stages in series/parallel.

All of them can essentially be viewed as variants of the first type, as shown below.

Noise matching to the source. The principle of noise matching to the signal source can be explained with the aid of Figure 26.12.

The sources v_n and i_n represent the equivalent amplifier input voltage and current noise, respectively. The purpose of the (ideal) transformer is to adjust the source impedance, as seen by the amplifier, in such a way that the available power of the equivalent noise source $v_{n,eq}$ becomes minimum. Since it leaves the equivalent power of the signal source v_s unchanged, this approach

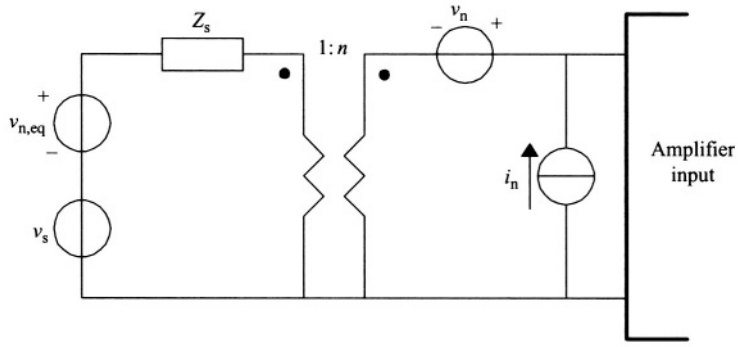

Figure 26.12. Principle of noise matching to the source.

maximizes the equivalent amplifier input SNR. The details are as follows. As known from circuit theory, the available power of v_s and $v_{n,eq}$ equals:

$$P_{av,v_s} = \frac{\bar{v}_s^2}{4\,\mathrm{Re}\{Z_s\}} \tag{26.4}$$

$$P_{av,v_{n,eq}} = \frac{\bar{v}_{n,eq}^2}{4\,\mathrm{Re}\{Z_s\}} \tag{26.5}$$

The equivalent amplifier input SNR equals the ratio of these two. The transformer has no effect on equation (26.4), but it does effect equation (26.5), through the relation between $v_{n,eq}$ and v_n, i_n:

$$v_{n,eq} = \frac{v_n}{n} + nZ_s i_n \tag{26.6}$$

Consequently, the amplifier input noise effectively "sees" a source impedance equal to $n^2 Z_s$. The transformation ratio n can now be chosen such that equation (26.5) is minimized, while equation (26.4) remains unchanged. For simplicity, assume that $Z_s = R_s$ is real, and v_n and i_n are uncorrelated (which is not always true). Then the optimal ratio n_{opt} satisfies:

$$n_{opt}^2 = \frac{1}{R_s}\sqrt{\frac{\bar{v}_n^2}{\bar{i}_n^2}} \tag{26.7}$$

A similar result is found if the signal source is a current source. For the optimal ratio, the contributions of v_n and i_n are equal. The advantage of this approach is that all noise sources in the amplifier are included in the optimization. The main disadvantage is that a transformer is not available in many cases or, as in microwave designs, realizes a match over a limited frequency range only.

Optimization of the bias current. This type of optimization [2,5] relies on the fact that the intensity of several transistor noise sources, the collector and base shot noise in a bipolar transistor and the channel noise in a MOS/JFET, depends on the transistor bias current. In addition, the chain parameters are also bias dependent.

The principle is illustrated by Figure 26.13, which depicts the nullor input stage with only the bias dependent noise sources.

The source $i_{n,1}$ represents the bias dependent output noise current source (collector shot noise/channel noise), present for both a bipolar and MOS/JFET input stage. As depicted, it transforms to the input through the chain parameters B and D. The bias dependent input noise source $i_{n,2}$ (base shot noise) is present only in case of a bipolar input stage. The power spectral density of both $i_{n,1}$ and $i_{n,2}$ is proportional to the transconductance g_m. Two different situations can be distinguished.

For a FET input stage, both B and D are proportional to $1/g_m$ and consequently, the power contents of all equivalent input noise sources due to $i_{n,1}$ is proportional to $1/g_m$. In this case, no global noise optimum exists; to minimize the noise g_m, that is, the bias current, should be chosen as large as possible.

For a bipolar input stage, a global noise optimum does exist. The chain parameter D is independent of g_m in this case, such that the power contents of the nullor input current noise is proportional to g_m. The power contents of the voltage noise are, similar to a FET input stage, proportional to $1/g_m$. The resulting possibility to optimize the noise with respect to g_m is very similar to optimization of the transformer ratio in the noise matching optimization, as illustrated by Figure 26.14.

The transistor at the right side is biased at a constant current $I_{c,o}$, resulting in a transconductance $g_{m,o}$. The total impedance seen from the transistor input,

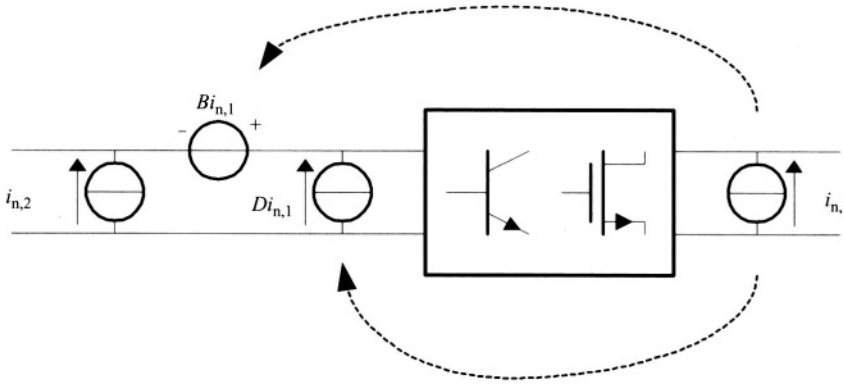

Figure 26.13. First nullor stage including bias dependent noise sources.

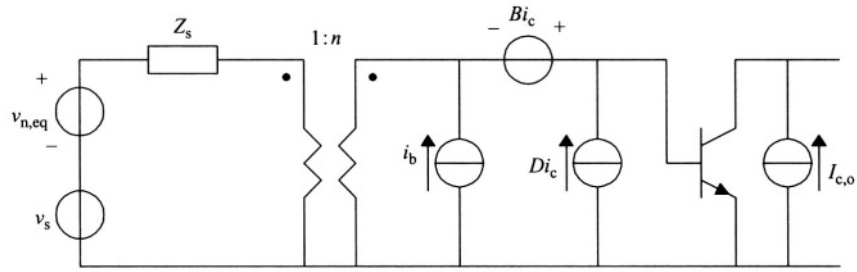

Figure 26.14. Similarity between noise matching and optimization of the bias current; the bias current changes the ratio of the (fictitious) transformer.

including the base resistance, is represented by Z_s. The fictitious transformer represents the effect of changing the bias current; the squared transformation ratio n^2 equals the factor by which this current and g_m are changed. It can be optimized in the same way as in the noise matching case. For example, when $Z_s = R_s$ is real, and $\beta_F \gg 1$ (such that Di_c is negligible compared to i_b), then it follows from equation (21.7) that:

$$n_{opt}^2 = \frac{g_m}{g_{m,o}} = \frac{1}{R_s}\sqrt{\frac{B^2\bar{i}_c^2}{\bar{i}_b^2}} = \frac{\sqrt{\beta_F}}{g_{m,o}R_s} \tag{26.8}$$

This is the familiar result for the g_m of an optimally biased bipolar input stage [3].

The strength of bias current optimization is that it is virtually always applicable; no additional circuitry is required. Its main disadvantage is the limited scope; it can only optimize the contribution of bias dependent sources such as i_c and i_b. The contribution of other sources cannot be affected by it.

Connecting stages in series/parallel. A third optimization method is connecting several input stages in series or in parallel/scaling of the input stage. Also, this approach can be explained with the aid of a fictitious transformer, as depicted in Figure 26.15.

If two identical stages are placed in parallel, their identical but uncorrelated input current sources add, resulting in a total noise current of $\sqrt{2}$ times the input current of a single stage. It can be shown that at the same time, the equivalent input noise voltage source of the two stages is *reduced* by a factor $\sqrt{2}$. In case of two series connected input stages, exactly the opposite situation occurs; the voltage noise increases by factor $\sqrt{2}$, while the current noise decreases by a factor $\sqrt{2}$. When n stages are placed in series or in parallel, the same magnification/reduction is observed, but now with a factor $\sqrt{n}$. Altogether, the effect of series/parallel connection is the same as that of a transformer with turn

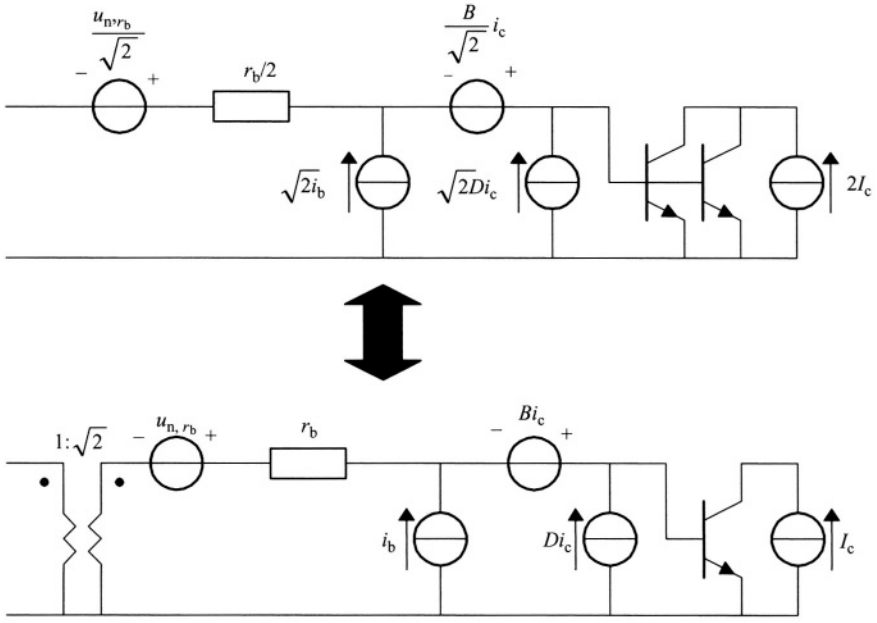

Figure 26.15. Effect of scaling or series/parallel connection of the nullor input stage. Depicted is a parallel connection of two identical CE-stages and its equivalent representation using a (fictitious) transformer.

ratio $\sqrt{n}$. Figure 26.15 shows the situation for parallel connection. For series connection, both ports of the transformer are interchanged.

The optimal scaling factor of the input stage can again be found from equation (26.7). In full-custom ICs, n can be chosen arbitrarily (within certain boundaries), but in semi-custom ICs and discrete circuits, only integer values can be realized.[1]

Summary of optimizations. Figure 26.16 shows all possible optimizations together in one amplifier. Bias current optimization has the most limited scope, since it only affects the noise sources that are dependent on the bias current (such as i_c and i_b), shown at the right of transformer 3. Placing stages in series/parallel (scaling) has a slightly wider scope; it also covers the bias independent noise sources of the input transistor, such as the noise of the base/gate resistance. It does not cover the noise produced by the feedback network. Furthermore, the turning ratio of the corresponding transformer, n_2, has to be

[1] Eventually, rational values for n can be obtained using combinations of series and parallel connection.

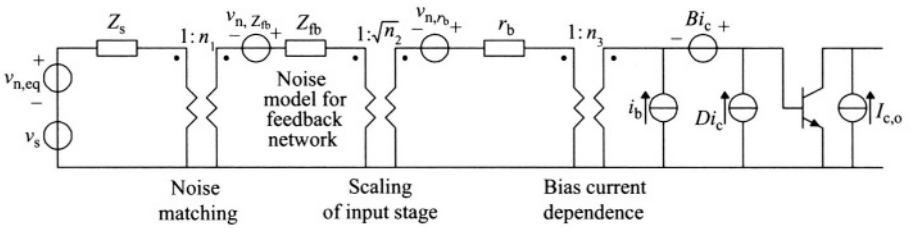

Figure 26.16. Summary of all possible amplifier noise optimizations.

integer (or rational) for discrete realizations. Noise matching to the source has the widest scope; it covers all noise produced by the amplifier, including the noise of the feedback network.

26.4. Low Noise Harmonic Resonator Oscillator Design

Another type of circuit is that which is encountered in a wide variety of electronic systems, where a frequency or timing reference is required, such as down-conversion in communication receivers, or as a clock in synchronous digital circuitry. In this section, we focus on low-noise design of an important subclass of oscillators; resonator oscillators. The characteristic property of these oscillators is that their frequency/time stability is determined by a passive, reactive component, such as an LC-tank or a crystal. As a consequence, they are intrinsically capable of attaining very low phase noise levels, and cannot be tuned over a wide range.

26.4.1. General Structure of a Resonator Oscillator

A resonator oscillator basically consists of two parts: a resonator and an undamping circuit, as depicted in Figure 26.17 [6–8].

The resonator serves as a frequency/timing reference, determining the oscillation frequency ω_o. Resonators with a high frequency stability are passive components that dissipate an extremely small, but noticeable amount of power. As a consequence, they are unable to sustain the oscillation autonomously. For this purpose, the undamping circuit is included; it supplies the energy dissipated by the resonator, such that the oscillation is maintained.

The dissipation inside the resonator, and the supply of energy by the undamping circuit are both fundamentally contaminated with noise. This noise, denoted by n_i in Figure 26.17, enters the oscillator loop and causes phase noise, that reduces the frequency stability. According to [9], the single-sideband phase noise power spectral density at a distance $\Delta\omega$ from the oscillation frequency

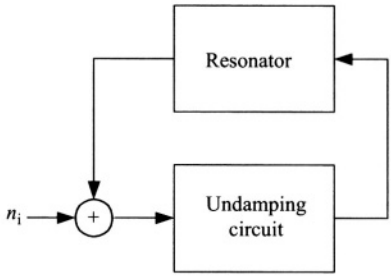

Figure 26.17. General structure of a resonator oscillator.

ω_o can be expressed as:

$$L(\Delta\omega) = \left(\frac{\omega_o}{\Delta\omega_o}\right)^2 \frac{S_{ni}(\omega_o + \Delta\omega_o)}{4Q^2A^2} \tag{26.9}$$

where A denotes the amplitude of the oscillation signal, S_{ni} the noise power density spectrum at the input of the undamping circuit and Q the quality factor of the resonator, defined as:

$$Q = \frac{\omega_o}{2}\left|\frac{d\phi(\omega)}{d\omega}\right|_{\omega=\omega_o} \tag{26.10}$$

where $\varphi(\omega)$ represents the resonator phase-frequency characteristic. Consequently, the minimum attainable phase noise level decreases proportionally to Q^2.

26.4.2. Noise Contribution of the Resonator

One of the contributions to the noise process n_i in Figure 26.17 is due to the dissipation of power in the resonator. In practice, various types of resonators are encountered in oscillators, varying from LC-tanks, to quartz crystals and even resonating sensor elements. From an electronic point of view, however, there are only two main classes: series resonators and parallel resonators, as depicted in Figure 26.18. Close to the resonance frequency, all resonators can be modeled as either a series or a parallel resonator [9,10]. In both models, the resistors represent the power loss in the resonators. As follows from thermodynamics, the noise produced by the resonators will, therefore, (at least) equal the thermal noise of these resistors.

The series resonator has a resonant voltage-to-current transfer (admittance with two complex poles). Therefore, for an oscillator constructed around such a resonator, the signal sensed at the input of the undamping circuit in Figure 26.17 is a current. The contribution of the resonator to the input noise n_i, therefore,

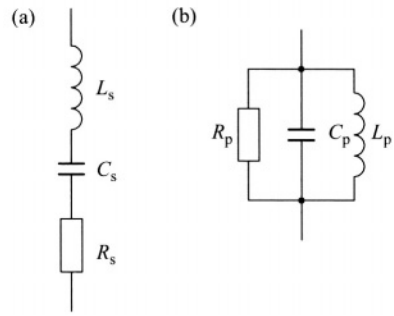

Figure 26.18. The two main resonator classes. (a) Series resonator and (b) parallel resonator.

equals the (thermal) noise current produced by R_s. Using equation (26.9) and [1., the corresponding minimum possible phase noise level is found to equal:

$$L_{s,\min}(\Delta\omega) = \frac{kTR_s}{A^2 L_s^2 (\Delta\omega)^2} \tag{26.11}$$

Thus, R_s should be as low as possible, or, equivalently, the quality factor $Q_s = \omega_o L_s / R_s$ should be as high as possible.

The parallel resonator has a resonant current-to-voltage transfer (impedance with two complex poles). Therefore, in an oscillator constructed around such a resonator, the signal sensed at the input of the undamping circuit in Figure 26.17 is a voltage. The contribution of the resonator to the noise n_i in this case equals the (thermal) voltage noise of R_p. The minimum phase noise level for this resonator equals:

$$L_{p,\min}(\Delta\omega) = \frac{kT}{A^2 R_p C_p^2 (\Delta\omega)^2} \tag{26.12}$$

Thus, in this case R_p should be as large as possible, which is also equivalent to an as large as possible quality factor $Q_p = \omega_o R_p C_p$.

Concluding, a low phase noise level can only be attained by using a resonator with a high quality factor.

26.4.3. Design of the Undamping Circuit for Low Noise

The purpose of the undamping circuit is to maintain the oscillation in the oscillator loop, by compensating for the power loss in the resonator. Since this power loss is modeled by the positive resistors R_s and R_p, the undamping circuit, exactly compensating the losses, can be represented by a negative resistance—R_s (series resonator) or —R_p (parallel resonator), as depicted for a series resonator in Figure 26.19.

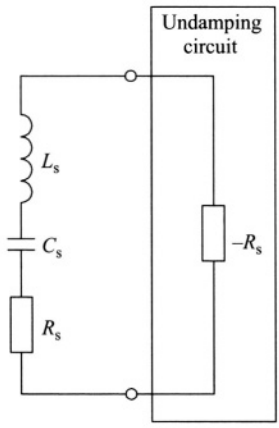

Figure 26.19. Undamping of a series resonator by a negative resistance.

In the remainder of the chapter, we concentrate on the series resonator; the results for the parallel resonator are easily derived from this by interchanging current and voltage.

Principle implementation of the undamping circuit. In principle, to sustain the oscillation, the undamping circuit in Figure 26.19 has to perform two operations:

- It has to sense the current through the resonator.
- It has to drive the voltage across the resonator.

Both functions can be performed by a transimpedance amplifier, as depicted in Figure 26.20.

To sustain the oscillation, the amplifier transfer should *exactly* equal the resonator series resistance R_s, which is impossible in practice. When the transfer is smaller than R_s, the oscillation will damp out, while it will grow unboundedly when the transfer is larger. Therefore, in order to stabilize the oscillation, an amplitude control loop is required that adjusts the amplifier gain to maintain a constant oscillation amplitude.

Amplitude control. The amplitude control can generally be realized in two different ways. The first possibility is to use a slow gain control loop that continuously adjusts the gain of the transimpedance amplifier. The second possibility is to replace the linear transimpedance amplifier by a limiting transimpedance amplifier. In that case, it has to be assured that the limiter gain exceeds the loss resistance R_s in order to maintain oscillation. Generally, the

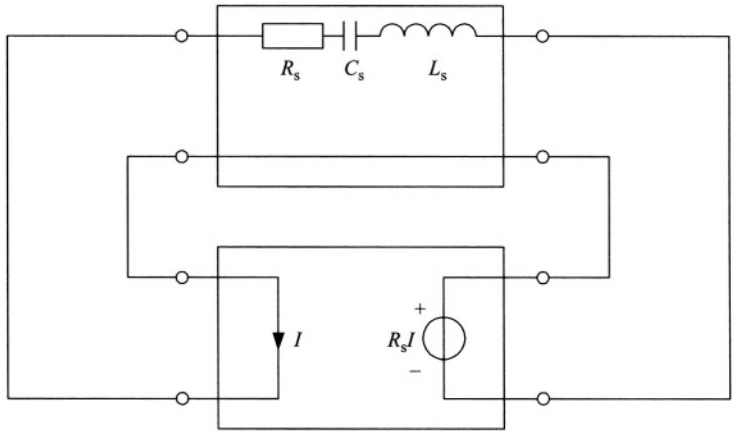

Figure 26.20. Implementation of a negative resistance by a transimpedance amplifier.

limiting amplifier solution is much simpler to implement and, as will be discussed below, only yields a slightly lower Carrier-to-Noise ratio (CNR) level than an ideal linear undamper.

Noise performance. Generally, two types of noise can be distinguished in an oscillator using a limiting amplifier as undamper:

- Noise with an intensity that is independent of time, such as the resonator noise and part of the amplifier noise.
- Noise with an intensity that switches "on" and "off".

An example of the latter type of noise is collector shot noise in a differential pair; when the differential pair saturates, the shot noise is not noticeable at the output ("off"), while it is noticeable in the linear region ("on"). The limiter gain can be used to realize a suitable trade-off between both types of noise. Aliasing due to the nonlinear transfer of the limiter increases the contribution of the first type of noise. This aliasing, and the noise, increases for increasing limiter gain values. In [10] is shown that a limiter "overdrive" of 2, that is, a gain of $2R_s$, is a suitable value that assures oscillation and degrades the CNR by only 3 dB due to aliasing. The contribution of the switching noise (second type) decreases for increasing limiter gain values; for increasing gain, the fraction of time that the limiter operates in its linear region decreases. The true optimum limiter gain value, therefore, depends on the relative magnitude of the switching noise and the continuous noise.

Driving the oscillator load. In principle, the undamping circuit can be combined with an output buffer/amplifier that drives the oscillator load. Such

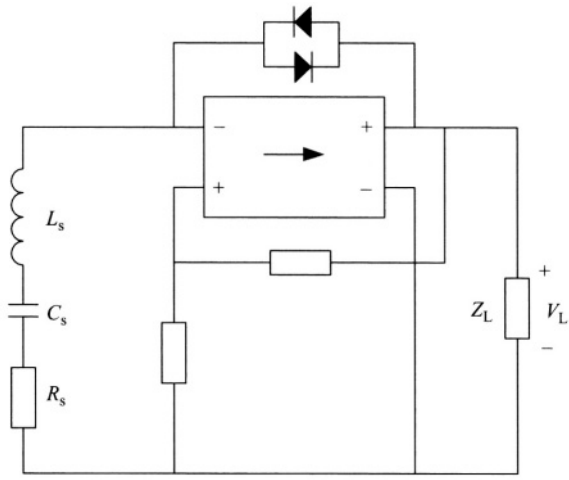

Figure 26.21. Oscillator with undamping realized by a double-loop limiting amplifier.

an amplifier is generally required to prevent so-called "loading" of the amplifier by the load, which reduces the resonator quality factor.

An elegant solution that comprises both the undamping and output buffering is provided by double-loop amplifier configurations. One negative and one positive feedback loop together realize an accurately defined, negative amplifier input impedance, and drive the load by an accurately defined voltage/current. An example of such a configuration, that establishes amplitude stabilization through limiting, is shown in Figure 26.21.

Further details on the design of double-loop undamping amplifier can be found in [10,11].

26.4.4. Noise Matching of the Resonator and Undamping Circuit: Tapping

In the same way as discussed for amplifiers, the noise behavior of the undamping circuit in resonator oscillators can be optimized using the techniques shown in Subsection 26.3.3. An especially useful optimization in oscillator design is noise matching to the source, which is the resonator in the oscillator case, as discussed below.

A simplified representation of the noise matching is depicted for a series resonator in Figure 26.22.

The voltage across the resonator is driven by the output of the amplifier (see Figure 26.20), which can be viewed as a short circuit. Close to the resonance frequency, the resonator behaves as a current source with source impedance R_S. The transformer can be used to minimize the equivalent amplifier input

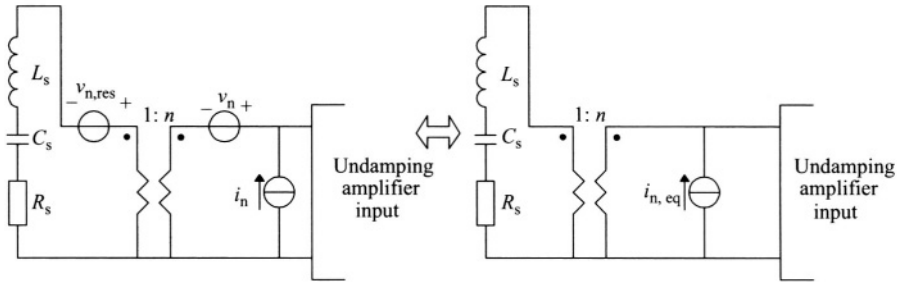

Figure 26.22. Noise matching to the resonator.

noise current $i_{n,eq}$ by matching R_s to the noise resistance R_n, the ratio of the rms value of v_n and i_n, of the amplifier. Seen from the amplifier input, the transformer enlarges the resonator series resistance to $n^2 R_s$. The equivalent amplifier input noise power can, therefore, be written as:

$$P_{n,eq} = n^2 R_s \bar{i}^2_{n,eq} = \frac{\bar{v}^2_{n,res}}{R_s} + \frac{\bar{v}^2_n}{n^2 R_s} + n^2 R_s \bar{i}^2_n \qquad (26.13)$$

The equivalent input signal power is independent of the transformer ratio n, such that the same optimum ratio as given by equation (26.7) is found again:

$$n^2_{opt} = \frac{1}{R_s}\sqrt{\frac{\bar{v}^2_n}{\bar{i}^2_n}} \qquad (26.14)$$

Obviously, for very high Q resonators, this optimum ratio can become impractically large. For medium and low Q resonators, the matching technique can provide a significant CNR improvement.

This matching technique wouldn't be interesting if there was no suitable means to approximate the ideal transformer. Fortunately, however, a suitable approximation technique does exist: capacitive (or inductive) tapping [9–12]. The principle is illustrated in Figure 26.23.

Besides the required transformer, the capacitive tap also adds an unwanted parallel capacitance. As long as the tapping capacitance C_2 is much smaller than C_1, that is, if the transformer ratio n is large, this parallel capacitance will have a negligible effect. Eventually, for relatively low transformation ratios, it will [11]:

1 add a parallel-resonance frequency above the series resonance frequency;

2 decrease the series resonance frequency;

3 degrade the Q factor.

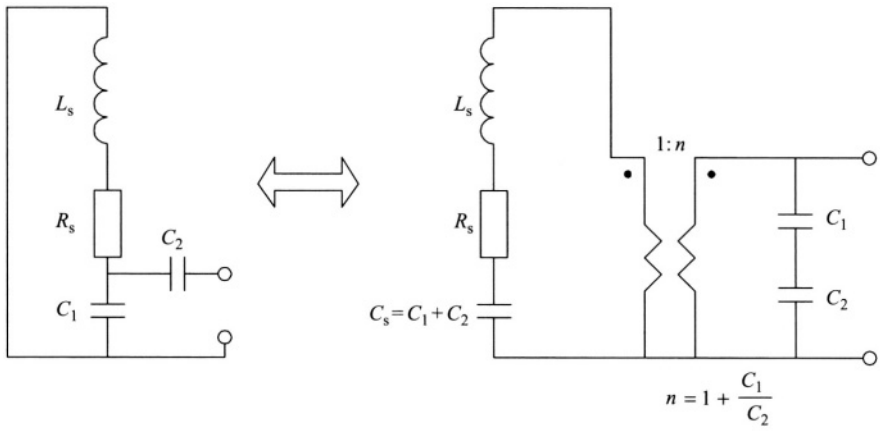

Figure 26.23. Approximation of a transformer by capacitive tapping.

When these effects occur, it is possible to cancel the parallel capacitance by means of an active negative capacitance [9,11], that in many cases can be incorporated in the design of the negative resistance/undamping amplifier. Details on the design on such negative capacitance can be found in [11].

26.4.5. Power Matching

Further optimization of the oscillator CNR, besides matching the undamping amplifier input to the source, is possible by power matching of the undamping amplifier output to its load [13]; the resonator. This power matching assures that the maximum possible power is delivered to the resonator (for a certain power consumption).

In principle, when the output impedance of the amplifier in Figure 26.20 is close to zero, it would be possible to deliver a very large amount of power to the resonator. However, for very high Q resonators, the current to be delivered by the amplifier to achieve this becomes extremely large. To reduce the required current, a transformer can be inserted, as depicted in Figure 26.24.

With this setup, the current through the resonator is n times as large as the current through the amplifier. Again, this transformer can be realized through capacitive tapping of the resonator. Consequently, if both noise matching and power matching is applied, we attain a configuration with a doubly tapped resonator, as depicted in Figure 26.25.

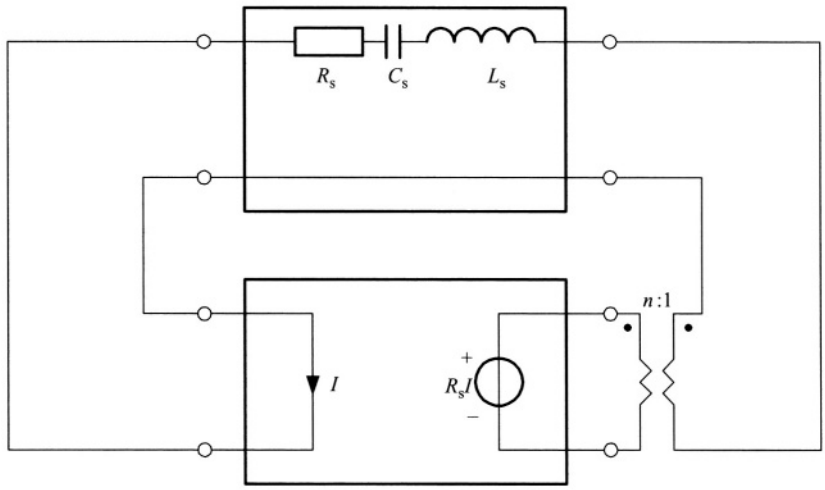

Figure 26.24. Power matching to reduce the amplifier output current.

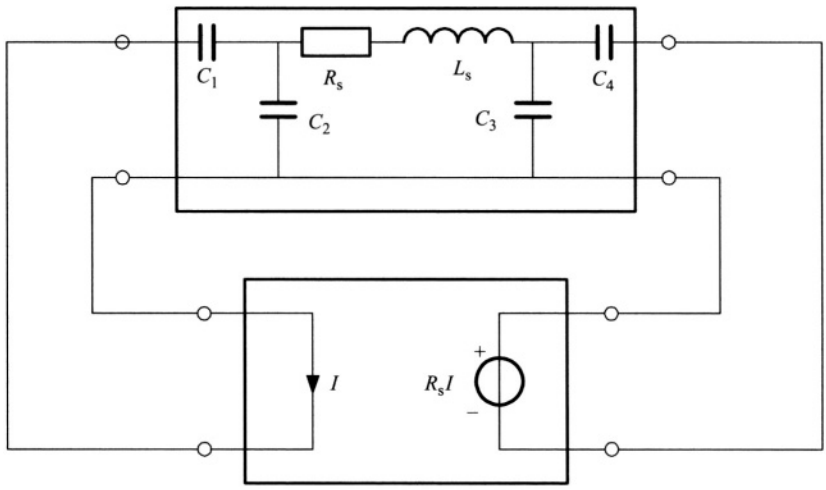

Figure 26.25. Doubly tapped resonator achieving both noise and power matching.

26.4.6. Coupled Resonator Oscillators

Besides selection of a high-Q resonator and the design of a low-noise undamping circuit, there is in principle a third possibility to minimize the phase noise; coupling several oscillators together. In literature, coupled resonator oscillators are proposed as means to achieve various objectives: a reduced phase noise level [14,15], an extended tuning range [16], and generation of

quadrature outputs [17,18]. Neither of these proposals, however, appears to be a very good solution [9]; resonator oscillators should not be coupled. In this section, we explain why coupling of resonator oscillators deteriorates the phase noise.

As expressed by equations (26.9) and (26.10), the phase noise level of a resonator oscillator is determined by the steepness (slope) of the resonator phase characteristic at the resonance frequency, that is, the frequency where the phase characteristic crosses through zero degrees. The steeper this characteristic is, the lower is the resulting phase noise level. Coupling deteriorates the phase noise level because it generally decreases the steepness of the phase characteristic, as discussed below. The ineffectiveness of coupling of resonator oscillators can be explained with the aid of the cascaded (in-phase coupled) structure of Figure 26.26.

Each resonator is accompanied by a separate undamping circuit to assure isolation of the resonators and prevent mutual loading effects (which deteriorate the resonator Q-factor). When all amplifiers and resonators are assumed to be identical, the total noise power in the loop equals N times the noise produced by a single resonator-amplifier combination (10 log(N) dB). At the same time, the steepness of the phase characteristic of the loop is N times larger than that of a single resonator. The combined effect of the noise and the slope of the phase characteristic is an improvement of the CNR by 10log(N) dB.

The conclusion that can be drawn from Figure 26.26 is that putting N identical resonators in cascade improves the phase noise by 101og(N) dB, at the cost of an N times higher power consumption. However, as shown by equation (26.9), the same improvement can be obtained by putting N times more power into a single resonator (if possible), that is, increasing the oscillation amplitude by a factor N^2. This already shows that coupling of resonator oscillators is a rather roundabout way to realize a CNR improvement of 10 1og(N) dB.

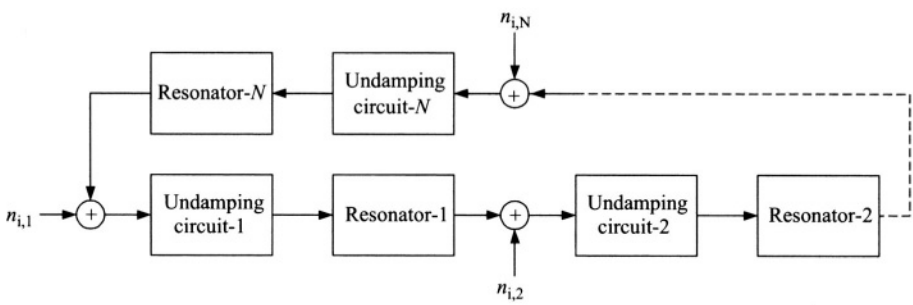

Figure 26.26. N cascade-coupled resonator oscillators.

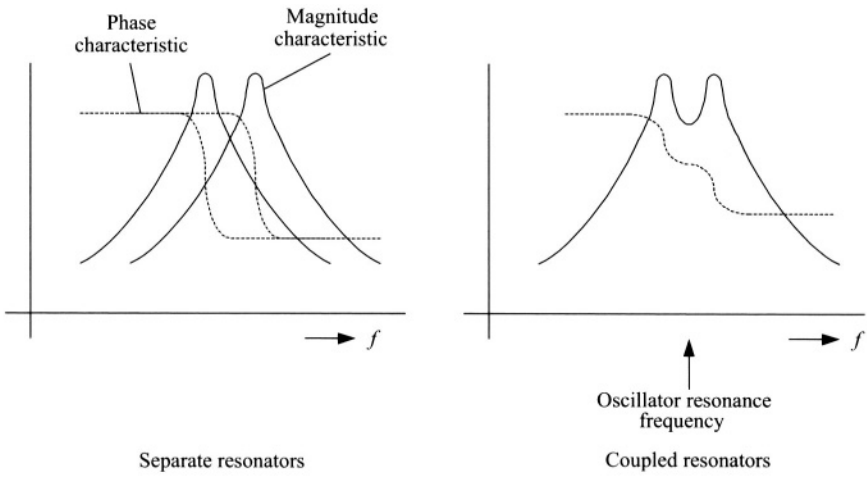

Figure 26.27. Magnitude and phase characteristics of separate resonators (left) and coupled resonators (right) with a slightly different resonance frequency.

In practice, the situation is actually far worse, because it is impossible to attain N exactly equal resonators with identical resonance frequencies. The oscillator resonance frequency will then be somewhere between the resonance frequencies of the individual resonators, where as illustrated by Figure 26.27, the slope of the loop's phase characteristic can even be much lower than that of a single resonator. Concluding, we observe that coupling of resonator oscillators is not only a roundabout way to put more power into the resonator, it is generally not a good solution.

26.5. Low-Noise Relaxation Oscillator Design

This section discusses the noise behavior of a second important class of oscillators; relaxation oscillators. These oscillators are also called "first-order" oscillators, because of the fact that, as opposed to, for example, a resonator oscillator, only one dynamic element, an integrator (usually a capacitor), determines the timing (frequency of oscillation). The differential equation describing their dynamic behavior, however, is of the second order.

Of course, a relaxation oscillator comprises more than just a single integrator. Figure 26.28 depicts a generalized block diagram, including the extra functions needed to implement a complete first-order oscillator. The capacitor integrates a constant current coming from the (binary) memory. When the detection level of one of the comparators is crossed, the memory is switched, its output changes sign and the integrator starts integrating towards the detection level of the other

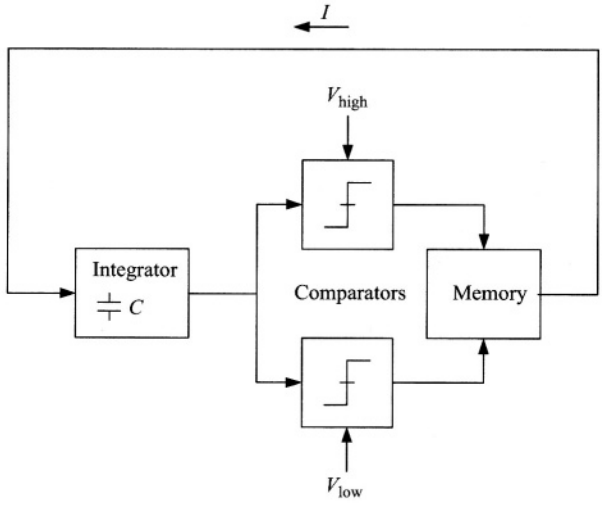

Figure 26.28. Generalized block diagram of a relaxation/first-order oscillator.

comparator. The frequency of oscillation is:

$$\omega_o = \frac{\pi}{(V_{high} - V_{low})C} \tag{26.15}$$

The operation of this class of oscillators is very basic and assumed to be known to the reader. More information on the basics can be found in [9,19].

The topology shown in Figure 26.28 is very commonly used. In this text we will take a close look at this topology to investigate its noise behavior and to consider the influence of the various components on the total noise behavior. We will see that alternative topologies, with a better noise performance do exist but are unfortunately rarely used.

26.5.1. Phase Noise in Relaxation Oscillators

When a relaxation oscillator is properly designed, which means that the right topology has been chosen and that the noise behavior has been optimized, its phase noise can be predicted via a rather simple equation. This is derived from the uncertainty involved with the point in time at which the integrator signal crosses the comparator detection levels. In this section, we discuss the modeling and causes of phase noise in relaxation oscillators. First, a simplified noise model is discussed. Subsequently, the influence of the memory and comparators on the phase noise is considered.

Simple phase noise model. In its simplest form, the noise in relaxation oscillators can be modeled by two noise sources. A noise current source (i_n) in

parallel to the output of the memory and a noise voltage source (v_n) in series with the capacitor. Depending on the frequency range occupied by the power spectral density of the noise sources, relative to the frequency of oscillation, different methods apply to calculate the resulting phase noise [9,19,20].

Noise that is (mainly) located at frequencies much smaller than the oscillation frequency ω_o causes frequency modulation of the oscillator, in the same way as a baseband message signal would do. Noise that is located at high frequencies, that is, around f_o and beyond, also noticeably influences the switching action of the comparators, which causes considerable noise aliasing. The aliased noise is located at low frequencies, and again causes frequency modulation of the oscillator.

If, for the moment, we assume that the aliasing noise is negligible, and that the power density spectra of i_n and v_n are white, the contribution of these sources to the oscillator phase noise power density spectrum equals:

$$L(\Delta\omega) = \frac{S_{i_n}}{2I^2}\left(\frac{\omega_o}{\Delta\omega}\right)^2 \tag{26.16}$$

$$L(\Delta\omega) = \frac{S_{v_n}}{(V_{high} - V_{low})^2}\left(\frac{\omega_o}{\Delta\omega}\right)^2 \tag{26.17}$$

The lower bound on the power density of v_n depends on the used technology. For a bipolar realization, this noise source is usually dominated by the thermal noise of the base resistance of the transistors.

Unfortunately, the noise aliasing effect is generally not negligible; the switching action is inherent to relaxation oscillators. High-frequency noise is folded back to low frequencies, causing low-frequency modulation of the oscillation signal. Aliased high-frequency noise components usually come from v_n, since the capacitor suppresses the high-frequency components of i_n. The effect of aliasing caused by v_n can be represented by a multiplication of its contribution to the phase noise, equation (26.17), by a factor:

$$\alpha = \frac{\pi B_{conv}}{\omega_o} \tag{26.18}$$

in which B_{conv} (in Hz) is the effective noise conversion bandwidth. In high-frequency oscillators, a dominant pole in the comparator usually determines B_{conv}.

Influence of the memory on the oscillator phase noise. The memory in a relaxation oscillator is a regenerative binary memory. It remembers the latest detection level that was crossed. This is the only task in a relaxation oscillator that cannot be done by another circuit. Another task that could be performed by the memory circuit, but also by other circuits is the comparator function. Any regenerative circuit is capable of detecting the crossing of

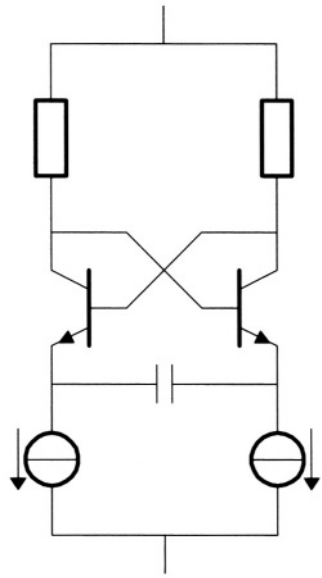

Figure 26.29. Emitter-coupled multi-vibrator; relaxation oscillator in which the memory also performs the level detection (comparator function).

a detection level by an input signal. This implies that, in principle, the comparators can be deleted from the topology depicted in Figure 26.28. The result is a very simple topology, implemented, for example, by the emitter-coupled multi-vibrator of Figure 26.29.

In order to evaluate the effect on the phase noise of omitting the comparators, the quality of the comparator function performed by the memory has to be analyzed. Figure 26.30 shows a plot of the state X of a regenerative circuit (memory) as a function of the memory input signal u_{in}. The z-shaped line connects the operating points at which the regenerative circuit is stable; it does not change state when it is on the line. When the operating point is not on the line, the memory changes state in the direction given by the block arrows in the graph. The graph shows two states: $-X_{\text{th}}$ and X_{th}. Between these states the memory has a regenerative behavior.

Outside the interval $X \in [-X_{\text{th}}, X_{\text{th}}]$ the memory is in a non-regenerative mode; the state variable X tracks the input signal u_{i} along the z-curve. The states $\pm X_{\text{th}}$ are the boundaries between the regenerative and the non-regenerative parts of the z-curve. Suppose that u_{i} increases from $-\infty$ towards positive values. The state variable X then follows the lower part of the z-curve, until it reaches $-X_{\text{th}}$ (a threshold state). If u_{i} increases any further, the memory enters its regenerative mode and X will move along transition T_1 to a point in

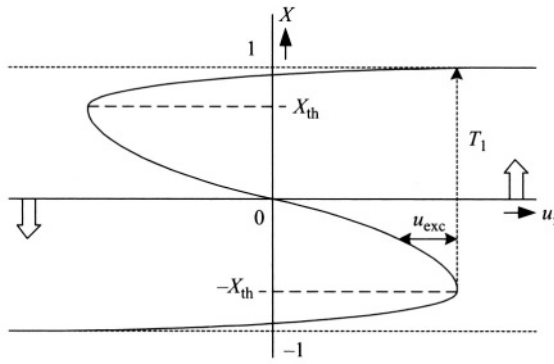

Figure 26.30. State of the regenerative (binary) memory as a function of the memory input signal u_{in}.

the other non-regenerative part of the z-curve, irrespective of the value of u_i. The stimulus that moves X to the other non-regenerative state can be quantified by the excitation (u_{exc}), the horizontal distance between the z-curve and the operating point of the memory circuit. From this it can be easily seen that when the transition starts, the excitation of the circuit is still very small, so the transition starts very slow and speeds up later. No matter what the amplitude of the input signal is, the excitation u_{exc} is only given by the distance of the operating point to the z-curve.

As a consequence, also effect of noise on the memory is determined by the (initially very low) SNR of the excitation u_{exc}, and *not* by the SNR of u_i. Therefore, a regenerative circuit can detect the crossing of a detection level, but only with extreme noise sensitivity and an initially slow reaction. The only way to improve this is to move the operating point quickly horizontally away from the z-curve (to the right), in order to stimulate the regenerative memory with an input signal that moves faster than the circuit can switch. This speeds up the start of the transition and makes it by far less noise sensitive. The topology shown in Figure 26.28, including the comparators, therefore, has a much better noise performance than the simpler topology of Figure 26.29. Further, it is not necessarily slower than the simple topology since the extra delay of the comparators can be very well compensated by acceleration of the state transition of the memory they introduce [21].

Influence of comparators on the oscillator phase noise. Above, it has been shown that the introduction of comparators in the relaxation oscillator is beneficial to the noise performance. However, there is also some risk involved in their use. How much gain should the comparators have, how fast should they be to improve the noise performance? Looking at Figure 26.28 again, it can

be seen that the comparators are embedded in a large *negative* feedback loop, that tries to keep the capacitor voltage below the detection levels. As soon as the capacitor voltage reaches detection level, the comparator starts generating a signal that "counteracts" this crossing. The comparator actually cancels its own stimulus, and the stimulus for the regenerative memory to switch state. The signal u_{in} in Figure 26.30 moves to the left again before the transition is completed. The only hope for the oscillator to function is that meanwhile, the excitation u_{exc} of the regenerative memory has gained sufficient strength to continue the state transition. Thus, although the trajectory Tl in Figure 26.30 may bend towards the z-curve, it should stay to the right of the curve. If it reaches the z-curve and crosses it due to a preliminary reduction of u_{in}, the regenerative memory returns to its original state and the oscillator stops.

Resistances in series with the integration capacitor increase the bandwidth of the negative feedback loop and, beyond certain resistance values, will also stop the oscillator. However, long before this happens, they make the oscillator even noisier than one would expect on the base of the noise contribution of the resistances themselves. Another way in which the bandwidth of the negative feedback loop is increased is by an increase of the gain of the comparators. Usually the introduction of comparators in a relaxation oscillator for level detection makes them less noisy [21]. It can, however, be easily seen that when the gain of the comparators would be infinite, the oscillator would "hang" at one of the detection levels. In practice, the combination of series resistances to the capacitor and the gain of the comparators increases the bandwidth of the negative feedback loop and thereby reduces the excitation of the regenerative memory somewhat. But as long as the increase of the excitation due to the comparators is larger than this reduction by the negative feedback loop, the introduction of the comparators is beneficial for the noise behavior. When the gain is increased further, the oscillator becomes more and more noisy and finally stops oscillating.

To prevent this effect from happening, the gain of the comparators should be kept low enough. The negative feedback loop, however, remains present, even in the absence of comparators, and always reduces the performance of the relaxation oscillator to some extent; it reduces the excitation of the regenerative memory. This loop, therefore, requires special attention in the design of relaxation oscillators.

26.5.2. Improvement of the Noise Behavior by Alternative Topologies

The main challenge for further improvement of the relaxation oscillator performance is to reduce the influence of the negative feedback loop or even remove it completely. In this section, two topologies will be shown that can be

used to achieve this. In the first topology, the regenerative memory is identified as the main "victim" of the feedback loop, and therefore the contribution of the memory to the overall timing of the oscillator is removed via a "memory bypass". In the second topology, which is a system of coupled relaxation oscillators, the loop is broken and its negative influence on the timing is thereby removed. Both topologies have shown to be very good candidates for low-noise relaxation oscillator designs [9,19,22].

Relaxation oscillators with memory bypass. When we look in detail at the various functions in relaxation oscillators, and evaluate the precise purpose of each of the components, it is observed that the only task for which the regenerative memory cannot be avoided is to remember which detection level was crossed last. In principle, it does not set the output frequency of the oscillator. The capacitor, the current that is integrated by the capacitor and the comparators that define the detection levels set the output frequency. This means that noise produced by the regenerative memory should not have influence on the oscillator output frequency.

Therefore, we can conclude that the topology shown in Figure 26.28, in which the memory actually is involved in the determination of the output frequency, is apparently not optimal. The regenerative memory cascades the comparators, such that its timing adds to the timing of the comparators. Its noise contribution is, therefore, also found in the output frequency. This effect is avoided in the topology depicted in Figure 26.31.

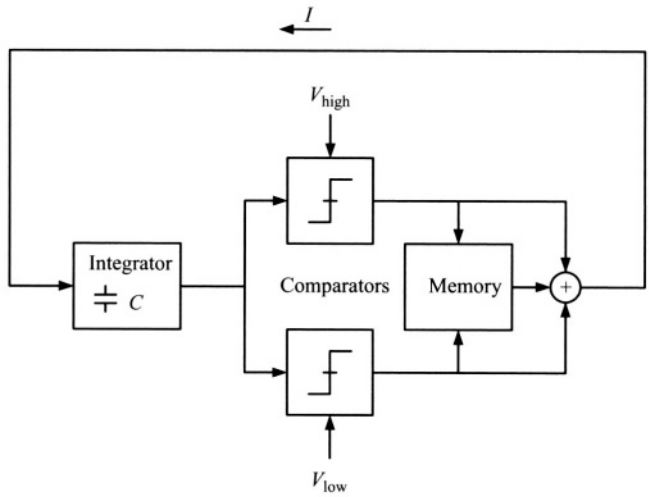

Figure 26.31. Relaxation oscillator with memory bypass [20].

There, regenerative memory does not cascade the comparators, but is put in parallel with them. The result of this is that around the state transitions, the comparators directly switch the integrator input current. At the same time the comparators stimulate the regenerative memory. The integration constant is thus already switching with a timing accuracy that is independent of the regenerative memory, the memory itself has the time to switch (in a noisy way) without injecting noise into the oscillator timing loop. The only restriction on the timing of the memory is that it should have reached its final state before the comparator stimulus disappears, due to the integrator signal that drops below the detection level again.

Figure 26.32 shows the various signals that appear in this topology. During the time that the integrator signal is above the detection level, the comparator output signal is high. The output signal of the memory, which is triggered by the comparators, follows later in time. Also shown by the combined signal is how the memory takes over from the comparator and keeps the signal level high after the comparator signal disappears again. The timing of the memory has little influence on the combined signal and thus the timing jitter of the memory is hardly contributing to the combined signal and with that to the output frequency of the oscillator.

Figure 26.33 shows a transistor circuit in which this topology has been implemented. Details on this circuit can be found in [9,20]. The center of the circuit diagram shows a flip-flop that fulfills the memory function. The differential pair above it is used as a current switch. The differential pairs at both sides of the flip-flop implement the comparator function. The differential pair

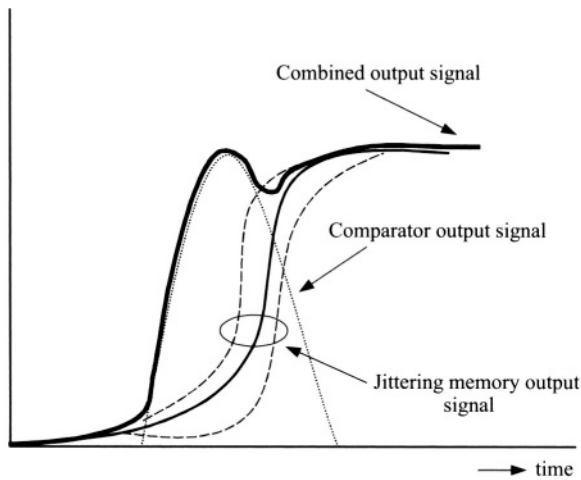

Figure 26.32. Signals in the "bypass" oscillator during a state transistion.

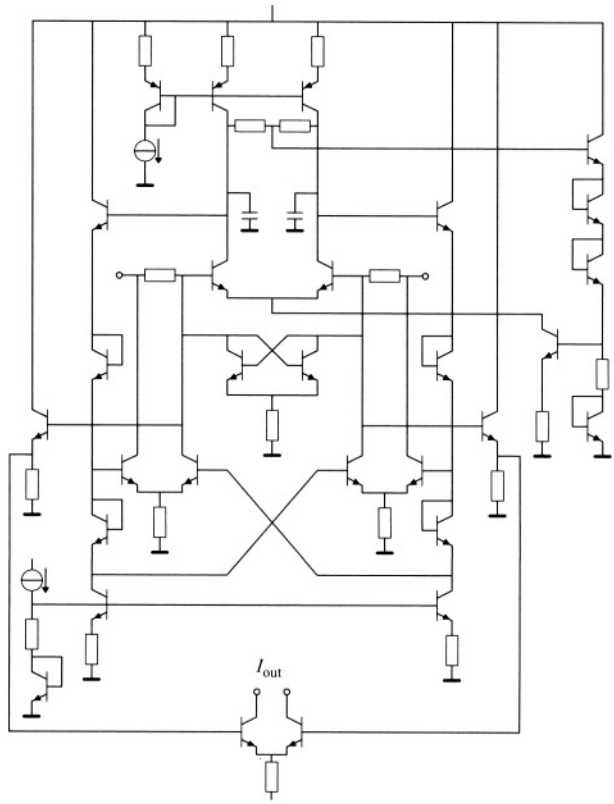

Figure 26.33. Relaxation oscillator with memory bypass [20].

at the bottom acts as an output buffer. All other transistors are used for biasing and level shift purposes. Two grounded capacitors have been used instead of one floating because the circuit has been integrated in a rather old IC-process in which capacitors have a large parasitic capacitor to the substrate at one plate. These plates are, therefore, chosen to coincide with the oscillator ground node, to make the parasites ineffective. The consequence of this is that the rest of the oscillator has to be floating, which explains the rather complicated biasing structure around the oscillator core. Clearly visible is that the comparators directly control the current switch. The flip-flop that is connected to the same node follows the signals and switches in parallel with the current switch without infecting the timing of the oscillator with its noise. When the comparator signal disappears again, the flip-flop keeps the current switch in the same state.

Coupled relaxation oscillators. *Quadrature coupling.* It has been previously discussed that the negative feedback loop in the oscillator reduces the

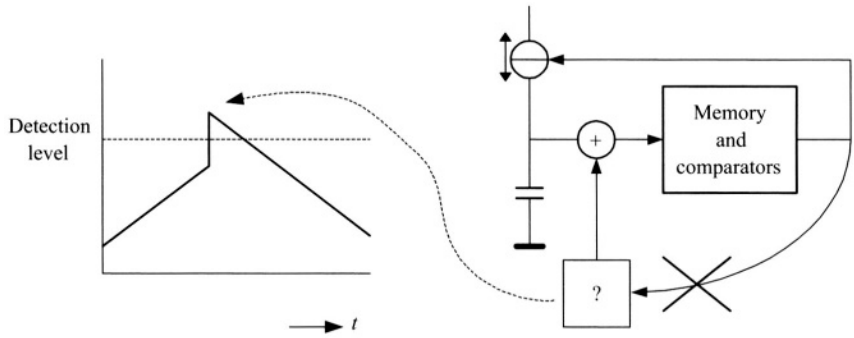

Figure 26.34. Configuration required to break the negative feedback loop around the detection level.

excitation of the regenerative memory. An improvement of the noise behavior of a relaxation oscillator can be expected when this loop is broken. The question, however is how to achieve this. Figure 26.34 illustrates the problem. To break the feedback loop when the capacitor (integrator) voltage in a relaxation oscillator approaches the detection level, the comparators should somehow quickly cross the detection level, as shown in Figure 26.34. In this way, there would be no chance for the feedback loop to counteract the comparator and memory input signals during the level crossing.

Unfortunately, such a situation cannot be realized through the comparators in the relaxation oscillator itself. Since they are also part of the negative feedback loop, increasing their gain to high values is detrimental to the noise behavior, as discussed before. Actually, it is difficult to derive the required "transition" signal directly from the oscillator itself. In fact, the only way to break the loop is to introduce a delay between the generation of such a signal and its actual addition to the capacitor voltage. However, since this delay will dominate the timing (and noise) behavior of the oscillator, it has to be very accurate and stable. It is unlikely that such a delay can be constructed with the same components available to implement the relaxation oscillator. If it were, possible, an oscillator would probably have been built around these components. Therefore, the only way to generate a delay that properly fits the requirements is to use a second relaxation oscillator. Figure 26.35 depicts the principle.

Figure 26.36 shows an implementation containing simple versions of relaxation oscillators; two emitter-coupled multi-vibrators. The quadrature coupling is realized by two differential pairs operating as limiters, depicted below the capacitors, that detect the zero crossings of the capacitor voltage and injected their output signal into the other oscillator. The mutual injection of zero crossings ensures that the two oscillators run in quadrature. The injected signals have

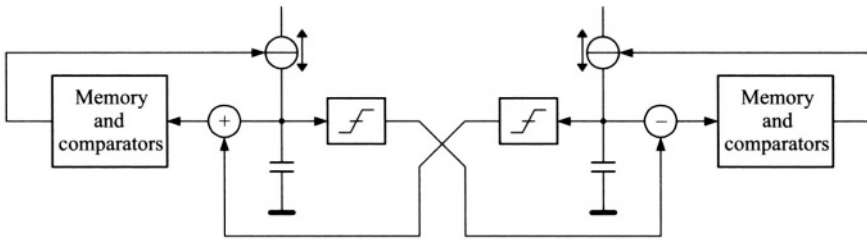

Figure 26.35. Breaking the negative feedback loop through quadrature coupling of two relaxation oscillators [9,19,23].

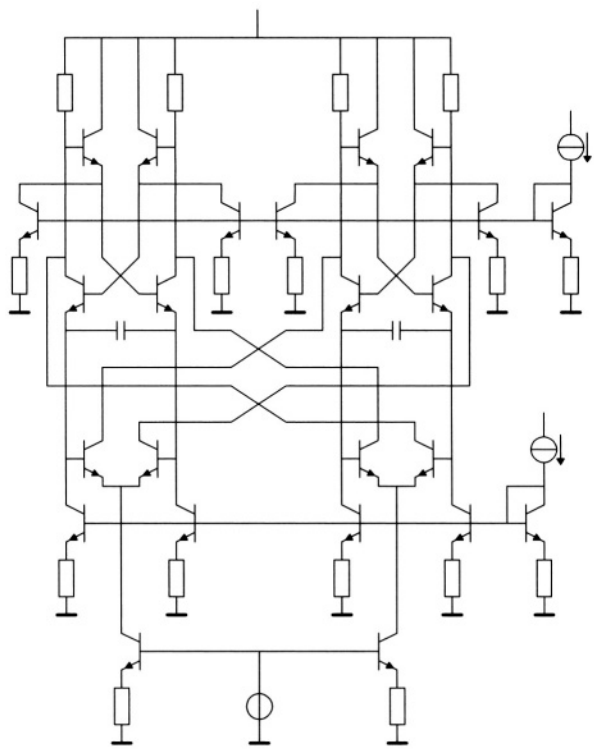

Figure 26.36. Implementation of a quadrature relaxation oscillator according to Figure 26.35.

no immediate timing relation to the switching of the oscillator; the negative feedback loop is broken. Due to this, the noise behavior of this topology is very good.

The extra feature of the topology, the fact that it produces nearly perfect quadrature signals, makes it extra attractive. The stability of the phase relation between the quadrature signals is far better than the absolute phase stability

of the system. It can be shown that the first-order sensitivity of the quadrature relation for noise equals zero [9]. To date, this topology seems to be the most accurate way to generate quadrature signals at the highest possible frequency, typically one-fifth of the f_T of the transistors; since no double frequency is needed to drive any dividers. Further, the quadrature relation is frequency independent since (frequency dependent) phase shifters are not used. Unlike the other methods to create quadrature signals, here is an active feedback mechanism that keeps the oscillators in quadrature, which is responsible for the extreme stability of the quadrature relation, without a compromise to the maximum operating frequency.

In-phase coupling. Another way to couple relaxation oscillators is *in-phase* coupling. Whereas quadrature coupling can only be applied to two oscillators, in-phase coupling can be applied to an arbitrarily large number of oscillators in parallel. The improvement of the noise behavior achieved in this way is not based on improvement of the excitation of the regenerative part, or by breaking the negative feedback loop, but on averaging. In a system of in-phase coupled relaxation oscillators, the oscillator that switches first initializes the switching of all other oscillators in the system. The average switching instant of the system is advanced and, more important, the variance of the switching instant is reduced.

Figure 26.37 shows how the noise behavior improves when the number of oscillators in the system is increased. For an increasing number of oscillators, the average of the state transition time reduces, while the distribution narrows. A system like this is very robust. A faulty oscillator would not hamper proper operation of the system. Large numbers of oscillators are needed to obtain a significant improvement. However, gradually, technology begins to offer the

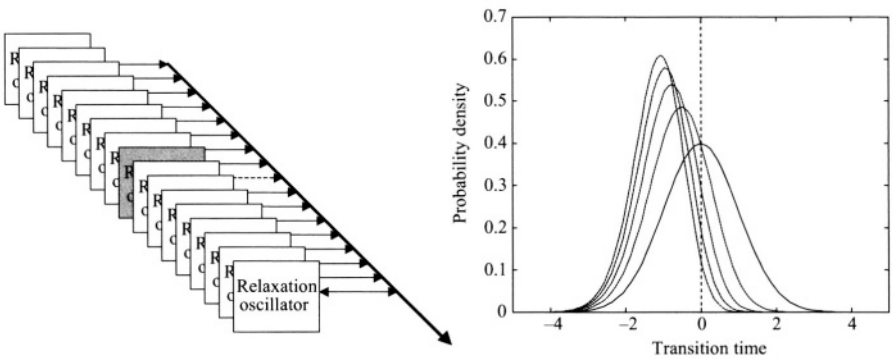

Figure 26.37. In-phase coupling of relaxation oscillators and probability density of the state transitions.

possibility to actually build systems like this. This type of oscillator systems can eventually attain the stability of a crystal oscillator, combined with the tuning range of a relaxation oscillator. There is no other oscillator topology to obtain this feature. Complex synthesizer systems also approach these characteristics, but they are more complicated to design, and much less robust. Nature shows many examples of in-phase coupled systems of relaxation oscillators, the hart muscle being one of the best known. Failure of one cell (relaxation oscillator) generally does not stop the hart. One could imagine what the changes of survival of a human being would be when the hart muscle had to rely on the pulses of one single clock-cell.

References

[1] G. A. M. van der Plas, J. Vandenbussche, W. Sansen, M. S. J. Steyaert and G. Gielen, "A 14-bit intrinsic accuracy Q^2 random walk CMOS DAC", *IEEE Journal of Solid-State Circuits,* vol. 34, no. 12, pp. 1708–1718, December 1999.

[2] E. H. Nordholt, *Design of High-Performance Negative Feedback Amplifiers.* Amsterdam: Elsevier, 1983.

[3] J. Davidse, *Analog Electronic Circuit Design.* Prentice Hall, New York, 1991.

[4] H. T. Friis, "Noise figures of radio receivers", *Proceedings of the IRE,* vol. 32, pp. 419–422, 1944.

[5] Z. Y. Chang and W. M. C. Sansen, *Low-Noise Wide-Band Amplifiers in Bipolar and CMOS Technologies.* Dordrecht: Kluwer Academic Publishers, 1991.

[6] A. A. Abidi, "How phase noise appears in oscillators", *Workshop on Advances in Analog Circuit Design,* Como, 1997.

[7] W. A. Edson, "Noise in oscillators", *Proceedings of the IRE,* vol. 48, pp. 1454–1466, 1960.

[8] D. B. Leeson, "A simple model of feedback oscillator noise spectrum", *Proceedings of the IEEE,* vol. 54, pp. 329–330, 1966.

[9] Jan R. Westra, Chris J. M. Verhoeven and Arthur H. M. van Roermund, *Oscillators and Oscillator Systems. Classification, Analysis and Synthesis.* Dordrecht: Kluwer Academic Publishers, 1999.

[10] C. A. M. Boon, "Design of high-performance negative feedback oscillators", Ph.D. thesis, Delft University of Technology, 1989.

[11] A. van Staveren, *Structured Electronic Design of High-Performance Low-Voltage Low-Power References,* Delft University Press, 1997.

[12] G. Braun and H. Lindenmeier, "Transistor oscillators with impedance noise matching", *IEEE Transactions on Microwave Theory and Techniques,* vol. 39, no. 9, pp. 1602–1610, September 1991.

[13] J. Craninckx and M. Steyaert, "Low-noise voltage-controlled oscillators using enhanced LC-tanks", *IEEE Transactions on Circuits and Systems-II,* vol. 42, no. 12, pp. 794–804, December 1995.

[14] M. M. Driscoll, "Low noise, VHF crystal-controlled oscillator utilizing dual, SC-cut resonators", *IEEE Transactions on Ultrasonics, Ferroelectrics, and Frequency Control,* vol. 33, no. 6, pp. 698–704, November 1986.

[15] Jae Joon Kim and Beomsup Kim, "A low-phase-noise CMOS LC oscillator with a ring structure", *ISSCC Digest of Technical Papers,* pp. 430–431, San Francisco, February 2000.

[16] N. M. Nguyen and R. G. Meyer, "A 1.8-GHz monolithic LC-voltage-controlled oscillator", *IEEE Journal of Solid-State Circuits,* vol. 27, no. 3, pp. 444–450, March 1992.

[17] A. A. Abidi, "A monolithic 900 MHz CMOS spread-spectrum wireless transceiver in 1-μm CMOS", *Proceedings of the Workshop on Advances in Analog Circuit Design,* Lausanne, Switzerland, 1996.

[18] A. Rofougaran, J. Rael, M. Rofougaran and A. A. Abidi, "A 900 MHz CMOS LC oscillator with quadrature outputs." *ISSCC Digest of Technical Papers,* San Francisco, 1996.

[19] C. J. M. Verhoeven, "First-order oscillators", Ph.D. thesis, Delft University of Technology, 1990.

[20] J. G. Sneep and C. J. M. Verhoeven, "A new low-noise 100-MHz balanced relaxation oscillator", *IEEE Journal of Solid-State Circuits,* vol. 25, pp. 692–698, 1990.

[21] A. A. Abidi and R. G. Meyer, "Noise in relaxation oscillators", *IEEE Journal of Solid-State Circuits,* vol. 18, no. 6, pp. 794–802, December 1983.

[22] C. J. M. Verhoeven, A. Van Staveren and J. R. Westra, "Low-noise oscillators", in: J. H. Huijsing et al. (eds), *Analog Circuit Design,* Dordrecht: Kluwer Academic Publishers, 1996.

[23] C. J. M. Verhoeven, "Coupled regenerative oscillator circuit", *US Patent 5,233,315,* 3 August 1993.